Superconductivity from doping boron icosahedra

Matteo Calandra
Laboratoire de Minéralogie-Cristallographie, case 115, 4 Place Jussieu, 75252, Paris cedex 05, France

Nathalie Vast
Laboratoire des Solides Irradiés, CEA-CNRS-Ecole Polytechnique, 91128 Palaiseau, France

Francesco Mauri
Laboratoire de Minéralogie-Cristallographie, case 115, 4 Place Jussieu, 75252, Paris cedex 05, France
(Received 8 December 2003; revised manuscript received 18 February 2004; published 15 June 2004)

We propose an alternative route to achieve the superconducting state in boron-rich solids, the hole doping of B_{12} icosahedra. For this purpose we consider a prototype metallic phase of $B_{13}C_2$. We show that in this compound the boron icosahedral units are mainly responsible for the large phonon frequencies logarithmic average, 65.8 meV, and the moderate electron-phonon coupling $\lambda = 0.81$. We suggest that this high T_c could be a general feature of hole-doped boron icosahedral solids. Moreover our calculated moderate value of λ excludes the formation of bipolarons localized on the icosahedral length scale as suggested by previous authors.

DOI: 10.1103/PhysRevB.69.224505 PACS number(s): 74.10.+v, 63.20.Dj, 63.20.Kr, 71.15.Mb

I. INTRODUCTION

Low-atomic-number elements have been intensively investigated in the attempt of finding electron-phonon-mediated superconductors with high critical temperatures (T_c). Boron-rich solids are eminent examples. The high-energy phonon frequencies of metallic boron layers in the structure of magnesium diboride[1] are mainly responsible for the 39 K T_c. Intercalation of these boron layers with lithium and boron substitution with carbon are currently under study[2] in the quest of even higher T_c. Elemental boron becomes metallic (maybe in a nonicosahedral structure[3,4]) and superconducting at 160 GPa, with a T_c which increases up to 11.2 K at 250 GPa.[3] A 23 K T_c has recently been discovered in intermetallic, yttrium palladium boron carbides.[5]

High-temperature superconductivity has been found in alkali-metal intercalated fullerene (C_{60}) and theoretically suggested in other intercalated carbon polyhedrons, C_{20},[6] C_{28},[7] or C_{36}.[8] C_{60} is a band insulator under normal conditions but the intercalation with alkali-metal atoms does generate a metallic state and a consequent superconducting state with T_c up to 40 K.[9] Superconductivity is mainly sustained by the high-frequency intramolecular phonons so that most of the physical properties of alkali-metal doped fullerenes can be understood from the solid C_{60} electronic and phonon structures. In particular it is seen that the small radius of the molecule substantially increases the electron-phonon coupling with respect to the case of the unrolled graphite layer.[10] The study of solids made of light atoms is then interesting since they can satisfy the two important requirements of having large phonon frequencies and fairly high electron-phonon coupling.

In this work we propose a different route to achieve the superconducting state in boron-rich solids, the hole doping of B_{12} icosahedra. For this purpose we consider a prototype metallic phase of $B_{13}C_2$ (Sec. II) for which we predict a T_c comparable to that of MgB_2. We show (Sec. III) that in this compound the boron icosahedral units are mainly responsible for the predicted large T_c. Thus this high T_c is a general feature of hole-doped boron icosahedral solids.

II. CRYSTAL STRUCTURE

We consider the hole doping of boron carbide $B_{12}C_3$ (or B_4C), a wide-gap band-insulator. Its crystal structure consists of an arrangement of $B_{11}C$ distorted icosahedra on the site of a rhombohedral lattice and of a linear C-B-C atom chain.[11–17] The periodic unit cell contains 15 atoms and is illustrated in Fig. 1. Hole-doped boron icosahedra can be naturally obtained replacing in $B_{12}C_3$ a carbon atom by a boron, giving $B_{13}C_2$. Due to the carbon substitution there is one hole per unit cell and, $B_{13}C_2$ being nonmagnetic, band theory predicts a metallic behavior. At zero temperature and ambient pressure however, $B_{13}C_2$ is a semiconductor.[18] The insulating character might be related to (i) the presence of structural defects[19,20] and (ii) Mott polaronic features.[21] In the first case a metallic state might be achieved simply by producing high-quality samples. In the second case it might be generated by the application of hydrostatic pressure in order to increase the hopping between the icosahedral units. The pressure necessary to metallize $B_{13}C_2$ would be lower than that necessary to metallize $B_{12}C_3$ or α-B. Indeed, the Mott-polaron gap in $B_{13}C_2$ is expected to be much smaller than the several eV gaps of the band insulators $B_{12}C_3$ and α-B.

The two most probable structures of $B_{13}C_2$ are $B_{11}C$(BBC), i.e., $B_{11}C$ icosahedra linked by BBC chains, or B_{12}(CBC), i.e., boron icosahedra linked by CBC chains. From the theoretical point of view, density functional theory (DFT) calculations[22] identified the B_{12}(CBC) structure as the most stable one with a 2.09 eV/cell larger binding energy with respect to $B_{11}C$(BBC). Experimentally[14] the ^{13}C NMR spectrum of $B_{13}C_2$ confirms the DFT calculations. Indeed changing composition from $B_{12}C_3$ to $B_{13}C_2$ the NMR peak associated with the C atom in the icosahedron disappears.

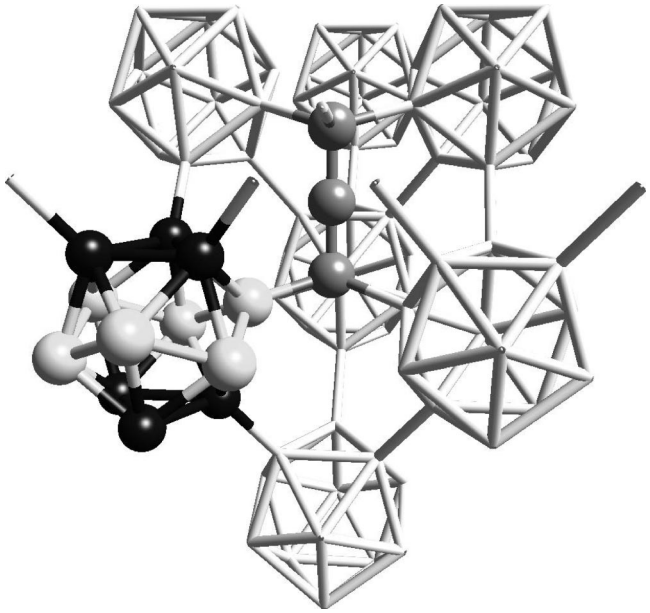

FIG. 1. Atomic structure of $B_{12}C_3$ and of $B_{13}C_2$. The black atoms are the polar sites, bonded to neighboring icosahedra. The white atoms are the equatorial sites. The gray atoms form the chain. In $B_{12}C_3$ the atoms in the chain are CBC and the icosahedra are $B_{11}C$ with the carbon placed in a polar site. In $B_{13}C_2$ the carbon atom in the polar site is replaced with a boron atom.

Therefore, in this paper, we use the B_{12}(CBC) structure and we refer to it as the $B_{13}C_2$ crystal structure. In other works it has been suggested that the substituted boron is on the chain.[23] We did not consider this proposed structure since we do not expect that the conclusions presented in this work are substantially affected by the location of the additional B atom.

III. CALCULATIONS AND RESULTS

In $B_{13}C_2$ a metallic phase could be achieved either by obtaining clean samples or by applying a small pressure. In DFT, already at room pressure, the ground state is metallic. Therefore we use DFT to study the superconducting properties of the hypothetical metallic state of $B_{13}C_2$. Electronic structure calculations[24] and geometrical optimization are performed using DFT in the local density approximation. We use norm-conserving pseudopotentials[25] with an *s* nonlocal part. The wave functions are expanded in plane waves using a 40 Ry cutoff. For the electronic structure we sample the Brillouin zone (BZ) using a $4\times4\times4$ Monkhorst-Pack grid (10 **k** points in the irreducible BZ wedge) and a first-order Hermite-Gaussian smearing of 0.03 Ry. From geometrical optimization we obtain the values of $a=9.686$ a.u. and $\alpha=66.05°$ for the cell parameters of the rhombohedral unit cell, very close to the experimental values[11] ($a=9.823$ a.u. and $\alpha=65.62°$).

The DFT band structure of $B_{13}C_2$ is shown in Fig. 2 and is in good agreement with Ref. 22. It displays a metallic behavior. The Fermi level is close to the top of the valence band and it is crossed by several bands. We calculated the electronic density of states (see Fig. 3) of $B_{13}C_2$, using a mesh of $N_k=14^3$ inequivalent **k** points. The mesh is generated by taking the mesh centered at the Γ point and shifting it by a random vector. The density of states at the Fermi level is $N(0)=3.6$ states per eV per unit cell. We decompose the $N(0)$ in icosahedral and chain density of states, by projecting the *ab initio* $B_{13}C_2$ wave function on the basis formed by the respective atomic pseudo-wave-function (Lowdin population).[26] At the Fermi level the icosahedral states are responsible for 88% of the total density of states [$N_{ico}(0)=3.2$]. In particular, the boron atoms in the polar sites have the largest contribution to $N_{ico}(0)$, namely, $N_{polar}(0)=2.3$ and the contribution due to the equatorial sites is smaller, $N_{eq}(0)=0.9$. Thus, most of the electrons involved in conduction processes resides in icosahedral states and only a small part in chain states [$N_{chain}(0)=0.4$].

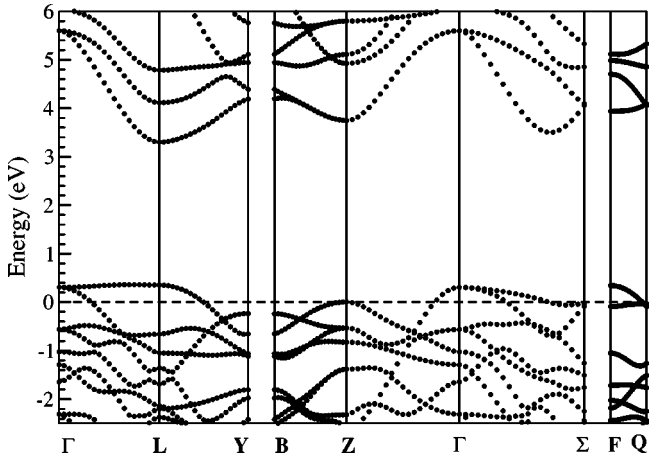

FIG. 2. DFT band structure of $B_{13}C_2$. The energy (eV) is referred to the Fermi energy level. The convention for high symmetry points in the Brillouin zone is from Ref. 30.

We compute the harmonic phonon frequencies $\omega_{\mathbf{q},\nu}$ using density functional perturbation theory in the linear

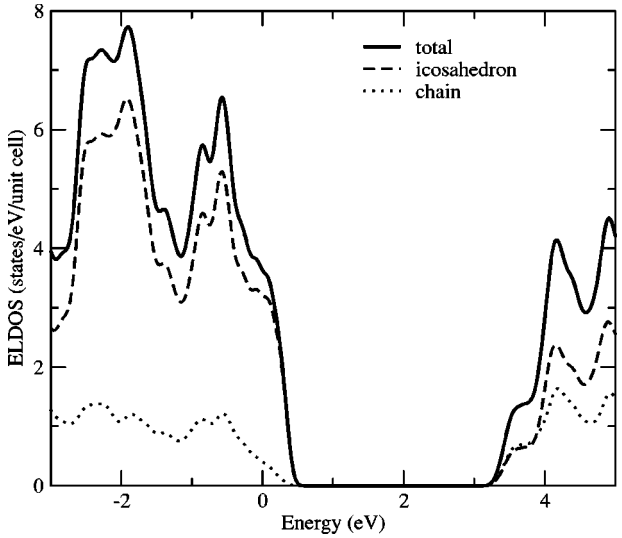

FIG. 3. DFT electronic density of states of $B_{13}C_2$ compared to the icosahedral atoms and chain atoms projected density of states. The energy (eV) is referred to the Fermi energy level.

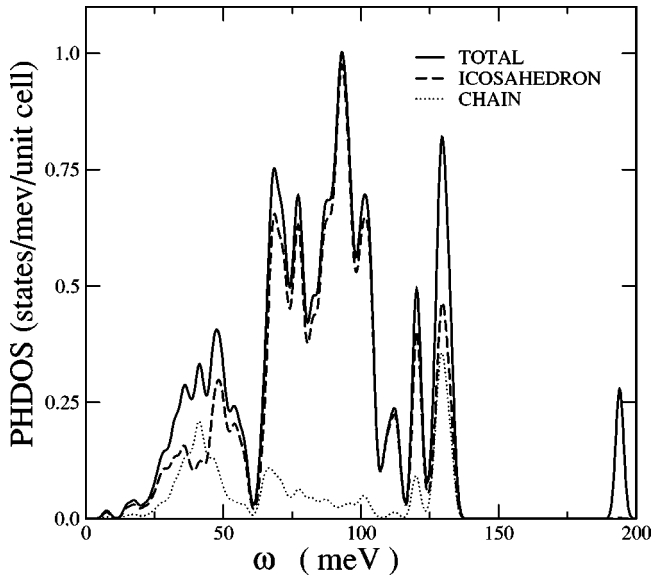

FIG. 4. Phonon density of states, $F(\omega)$, of $B_{13}C_2$. The total density of states (solid line) compared to the phonon density of states of the icosahedral modes (dashed line) and of the chain modes (dotted line). Most of the weight between 0 and 140 meV is due to icosahedral modes.

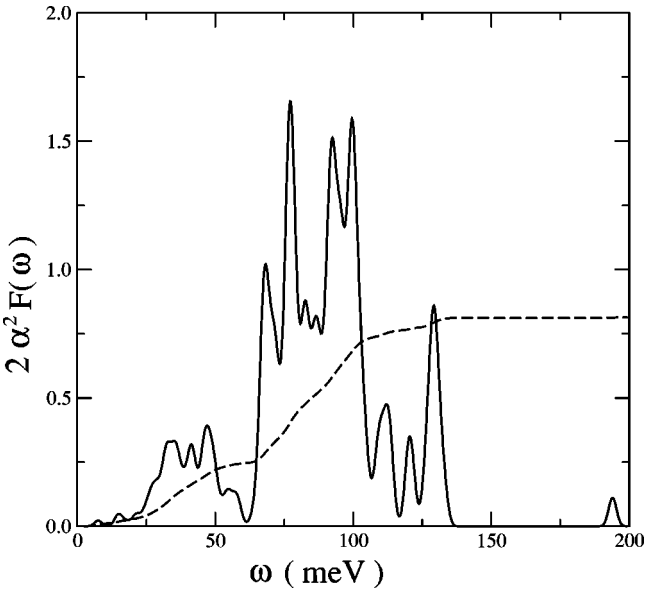

FIG. 5. Eliashberg function (solid line) and average electron-phonon coupling (dashed line) of $B_{13}C_2$. The icosahedral phonon modes ranging between 60 and 105 meV give the largest contribution to λ.

response.[24] We use a $N=4^3$ Monkhorst-Pack **q**-point mesh, **q** being the phonon wave vector. The total phonon density of states, $F(\omega)$, together with the phonon density of states restricted to the icosahedral and chain phonon modes, are shown in Fig. 4. The large number of peaks in $F(\omega)$ is determined by the large number of phonon modes present in the system.

The icosahedral phonon modes are responsible for most of the weight between 0 and 140 meV. The vibrations of the atoms in the chain explain the high-energy feature at 193 meV (both B and C vibrations) and part of the feature at 129 meV (C vibrations). The structures in the chain restricted $F(\omega)$ between 25 and 55 meV are mainly due to B vibrations, while the remaining weight between 60 and 106 meV is due to C vibrations.

The electron-phonon interaction for a phonon mode ν with momentum q can be written as

$$\lambda_{\mathbf{q}\nu} = \frac{4}{\omega_{\mathbf{q}} N(0) N_k} \sum_{\mathbf{k},n,m} |g^{\nu}_{\mathbf{k}n,\mathbf{k}+\mathbf{q}m}|^2 \delta(\varepsilon_{\mathbf{k}n}) \delta(\varepsilon_{\mathbf{k}+\mathbf{q}m}), \qquad (1)$$

where the sum is carried out over the BZ, and $\varepsilon_{\mathbf{k}n}$ are the energy bands measured with respect to the Fermi level at point **k**. The matrix element is $g^{\nu}_{\mathbf{k}n,\mathbf{k}+\mathbf{q}m} = \langle \mathbf{k}n | \delta V / \delta u_{\mathbf{q}\nu} | \mathbf{k}+\mathbf{q}m \rangle / \sqrt{2\omega_{\mathbf{q}\nu}}$, where $u_{\mathbf{q}\nu}$ is the amplitude of the displacement of the phonon ν of wave vector **q**, V is the Kohn-Sham potential, and $N(0)=3.6$ states per eV per unit cell is the electronic DOS at the Fermi level. The electron-phonon coupling λ is then calculated as an average over the N **q**-point mesh and over all the modes, $\lambda = \Sigma_{\mathbf{q}\nu} \lambda_{\mathbf{q}\nu} / N = 0.81$.

The modes responsible for superconductivity can be identified from the Eliashberg function $\alpha^2 F(\omega)$:

$$\alpha^2 F(\omega) = \frac{1}{2N} \sum_{\mathbf{q}\nu} \lambda_{\mathbf{q}\nu} \omega_{\mathbf{q}\nu} \delta(\omega - \omega_{\mathbf{q}\nu}). \qquad (2)$$

The Eliashberg function is depicted in Fig. 5. Most of the contribution to λ comes from the region from 60 to 105 meV, mainly related to the icosahedral phonon modes.

The critical superconducting temperature is estimated from the calculated phonon frequencies and electron-phonon coupling using the McMillan formula:[27]

$$T_c = \frac{\langle \omega \rangle}{1.2} \exp\left(- \frac{1.04(1+\lambda)}{\lambda - \mu^*(1+0.62\lambda)} \right), \qquad (3)$$

where μ^* is the screened Coulomb pseudopotential that takes into account the Coulomb repulsion between the electrons dressed by retardation effects due to the phonons and $\langle \omega \rangle = 65.8$ meV is the phonon frequency logarithmic average. The calculated values of T_c for $B_{13}C_2$ as a function of μ^* are illustrated in Table I. The critical temperature for metallic $B_{13}C_2$ is comparable to the one obtained for MgB_2 and, using

TABLE I. Critical temperatures of $B_{13}C_2$ and MgB_2. Predicted critical temperatures as a function of the screened Coulomb pseudopotential (μ^*). The critical temperature is estimated using the McMillan formula [Eq. (3)]. The results are compared with MgB_2 (from Ref. 31).

Material	μ^*	$\langle \omega \rangle$ (meV)	λ	T_c (K)
$B_{13}C_2$	0.1	65.8	0.81	36.7
	0.14	65.8	0.81	27.6
	0.2	65.8	0.81	15.8
MgB_2	0.14	62.0	0.87	30.7

the McMillan formula, ranges between 15.8 and 36.7 K.

Our calculation of the electron-phonon coupling gives also new insight on the possible occurrence of a bipolaronic insulating state in $B_{13}C_2$, as suggested by other authors.[21] In icosahedral boron compounds the bipolaron could be localized on two length scales: the icosahedron length scale or a smaller one, of the order of the bond length. If the bipolaron were localized on the icosahedron length scale (as most of the bipolaronic literature seems to suggest[21]) the bipolaronic distortion could be seen as a small perturbation to the metallic state. In this case the bipolaron could be described within a model considering a linear electron-phonon coupling perturbation to the harmonic Hamiltonian in the metallic phase. Such a model is the one used in the present paper to study the superconducting properties. Our calculated value of λ is too small[28] to justify a bipolaronic insulating state for $B_{13}C_2$. In contrast our calculation cannot exclude the occurrence of a bipolaron localized on the bond-length scale. In this scenario the bipolaron would involve a substantial deformation of our crystal structure (e.g., the breaking or formation of chemical bonds). Such a strong deformation could not be seen as a weak perturbation to the harmonic Hamiltonian in the metallic state and could not be described by the approach used in the present paper.

IV. CONCLUSIONS

In this work we have studied the possible occurrence of superconductivity from hole-doping boron icosahedra. We found the possibility of having high superconducting critical temperatures in these systems. As a possible physical realization of a metallic state we have considered $B_{13}C_2$, which is formed from B_{12} icosahedral units with one hole per icosahedra. Using *ab initio* calculations we have determined its normal state properties, finding a moderate electron-phonon coupling and a large phonon logarithmic average to the phonon frequencies. We have demonstrated that both properties are connected to the B_{12} building blocks. Indeed the local density of state at the Fermi level and the phonon modes strongly coupled with electrons are localized on the icosahedra. As a consequence our findings are not restricted to $B_{13}C_2$ compounds but can be applied to other metallic compounds composed by B-rich icosahedra. For example, another possibility to achieve a metallic state is the substitution of P with Si in $B_{12}P_2$ or of As with Si in $B_{12}As_2$. $B_{12}P_2$ and $B_{12}As_2$ are band insulators composed of B_{12} icosahedra and two-atom P_2 or As_2 chains.[23] The substitution of pentavalent atoms such as As and P with tetravalent Si introduces a hole in the system. $B_{12}P_{2-x}Si_x$ wafer resistivity measurements show a low electrical conductivity.[29] If such conduction were related to bipolaron formation, then a metallic state could be achieved by applying pressure. An advantage of the two-atom chain systems ($B_{12}P_{2-x}Si_x$ or $B_{12}As_{2-x}Si_x$) with respect to the three-atom chain systems ($B_{13}C_2$) is the lack in the formers of an internal soft degree of freedom, the chain bending. Probably this feature makes the two-atom chain structures more stable under pressure.

ACKNOWLEDGMENTS

We acknowledge illuminating discussions with M. Bernasconi, P. Giannozzi, and E. Tosatti. We thank C. J. Pickard for providing us the figure of the molecular structure. Computer time has been granted by IDRIS (project 000544 and 021202). M.C. was supported by a Marie Curie Fellowship of the European Commission, Contract No. IHP-HPMF-CT-2001-01185.

[1] J. Nagamatsu, N. Nakagawa, T. Muranaka, Y. Zenitani, and J. Akimitsu, Nature (London) **410**, 63 (2001).

[2] H. Rosner, A. Kitaigorodsky, and W. E. Pickett, Phys. Rev. Lett. **88**, 127001 (2002).

[3] M. I. Eremets, V. V. Struzhkin, H. Mao, and R. J. Hemley, Science **293**, 272 (2001).

[4] D. N. Sanz, P. Loubeyre, and M. Mezouar, Phys. Rev. Lett. **89**, 245501 (2002).

[5] R. J. Cava, H. Takagi, B. Batlogg, H. W. Zandbergen, J. J. Krajewski, W. F. Peck, R. B. van-Dover, R. J. Felder, T. Siegrist, K. Mizuhashi, J. O. Lee, H. Eisaki, S. A Carter, and S. Uchida, Nature (London) **367**, 146 (1994).

[6] I. Spagnolatti, M. Bernasconi, and G. Benedek, Europhys. Lett. **59**, 572 (2002); **60**, 329 (2002).

[7] N. Breda, R. A. Broglia, G. Colò, G. Onida, D. Provasi, and E. Vigezzi, Phys. Rev. B **62**, 130 (2000).

[8] P. G. Collins, J. C. Grossman, M. Côté, M. Ishigami, C. Piskoti, S. G. Louie, M. L. Cohen, and A. Zettl, Phys. Rev. Lett. **82**, 165 (1999).

[9] O. Gunnarsson, Rev. Mod. Phys. **69**, 575 (1997).

[10] M. Schluter, M. Lannoo, M. Needels, and G. A. Baraff, Phys. Rev. Lett. **68**, 526 (1992).

[11] A. Kirfel, A. Gupta, and G. Will, Acta Crystallogr., Sect. B: Struct. Crystallogr. Cryst. Chem. **35**, 1052 (1979).

[12] A. C. Larson, in *Boron-Rich Solids*, edited by D. Emin, T. L. Aselage, C. L. Beckel, I. A. Howard, and C. Wood (AIP, New York, 1986), p. 109; B. Morosin, T. L. Aselage, and R. S. Feigelson, Mater. Res. Soc. Symp. Proc. **97**, 145 (1987).

[13] D. R. Tallant, T. L. Aselage, A. N. Campbell, and D. Emin, Phys. Rev. B **40**, 5649 (1989).

[14] R. J. Kirkpatrick, T. Aselage, B. L. Phillips, and B. Montez, in *Boron-Rich Solids*, edited by D. Emin, T. L. Aselage, A. C. Switendick, B. Morosin, and C. L. Beckel (AIP, New York, 1991).

[15] U. Kuhlmann, H. Werheit, and K. A. Schwetz, J. Alloys Compd. **189**, 249 (1992).

[16] R. Lazzari, N. Vast, J. M. Besson, S. Baroni, and A. Dal Corso, Phys. Rev. Lett. **83**, 3230 (1999); **85**, 4194 (2000).

[17] F. Mauri, N. Vast, and C. J. Pickard, Phys. Rev. Lett. **87**, 085506 (2001).

[18] R. Kormann and L. Zuppiroli, in *Boron-Rich Solids*, edited by D. Emin, T. L. Aselage, C. L. Beckel, I. A. Howard, and C. Wood (AIP, New York, 1986), p. 216; N. Papandreou and L. Zuppiroli, Ref. 14, p. 85.

[19] P. Favia, T. Stoto, M. Carrard, P. A. Stadelmann, and L. Zuppiroli, Microsc. Microanal. Microstruct. **7**, 225 (1996); B. Wei, R. Vajtai, Y. J. Jung, F. Banhart, G. Ramanath, and P. M. Ajayan, J. Phys. Chem. B **106**, 5807 (2002).
[20] F. Thevenot, J. Eur. Ceram. Soc. **6**, 205 (1990).
[21] T. L. Aselage, D. Emin, and S. S. McCready, Phys. Rev. B **64**, 054302 (2001).
[22] D. M. Bylander and L. Kleinman, Phys. Rev. B **43**, 1487 (1991).
[23] T. L. Aselage, D. R. Tallant, and D. Emin, Phys. Rev. B **56**, 3122 (1997).
[24] S. Baroni, S. de Gironcoli, and A. Dal Corso, Rev. Mod. Phys. **73**, 515 (2001).
[25] N. Troullier and J. L. Martins, Phys. Rev. B **43**, 1993 (1991).
[26] D. Sanchez-Portal, E. Artacho, and J. M. Soler, Solid State Commun. **95**, 685 (1995).
[27] W. L. McMillan, Phys. Rev. **167**, 331 (1968).
[28] S. Robaszkiewicz, R. Micnas, and K. A. Chao, Phys. Rev. B **23**, 1447 (1981).
[29] Y. Kumashiro, T. Yokohama, K. Sato, Y. Ando, S. Nagatani, and K. Kajiyama, J. Solid State Chem. **154**, 33 (2000).
[30] C. J. Bradley and A. P. Cracknell, *The Mathematical Theory of Symmetry in Solids* (Clarendon Press, Oxford, 1972).
[31] Y. Kong, O. V. Dolgov, O. Jepsen, and O. K. Andersen, Phys. Rev. B **64**, 020501(R) (2001).